Available online at www.sciencedirect.com

SciVerse ScienceDirect

Ceramics International 38 (2012) 3243–3250

CERAMICS INTERNATIONAL

www.elsevier.com/locate/ceramint

Si-SiC-ZrB_2 ceramics by silicon reactive infiltration

Alberto Ortona [a,*], Paolo Fino [b], Claudio D'Angelo [a], Sara Biamino [b], Giuseppe D'Amico [b], Daniele Gaia [c], Sandro Gianella [c]

[a] *ICIMSI-SUPSI, Strada Cantonale, CH-6928, Manno, Switzerland*

[b] *Politecnico di Torino, Dipartimento di Scienza dei Materiali e Ingegneria Chimica, Torino, Italy*

[c] *Erbicol SA, Viale Pereda, 21, CH-6228, Balerna, Switzerland*

Received 28 October 2011; received in revised form 14 December 2011; accepted 15 December 2011
Available online 23 December 2011

Abstract

Silicon carbide ceramics obtained by silicon reactive infiltration are nowadays employed within industry in several high temperature applications. Although these ceramics show good thermo-mechanical properties and oxidation resistance, they suffer temperature limitations (1400 °C). At higher temperatures another type of ceramics, commonly known as ultra high temperature ceramics (UHTCs), is under study. These include the transition metal diborides of group IV; one in particular, zirconium diboride, is interesting in certain applications (e.g. aerospace) because of its low relative density. ZrB_2-SiC ceramics show good thermo-mechanical properties and maintain the ''protective'' passive oxidation regime of their scales over a wide range of temperatures.

This paper presents a feasibility study on a manufacturing methodology to produce Si-SiC-ZrB_2 bulk ceramics taking advantage of the reactive infiltration technique. This technique allows lower processing temperatures and near to net shape capability due to low shrinking of the green compacted bodies. C-SiC-ZrB_2 preforms were successfully infiltrated with molten silicon. The resulting Si-SiC-ZrB_2 composites showed promising oxidation behavior, similarly to that reported in other works. Bulk material optimization was performed with a view to manufacturing Si-SiC-ZrB_2 ceramic matrix composites by silicon reactive infiltration in future.

Keywords: Carbides; Borides; Reaction bonding; Oxidation behavior

1. Introduction

Molten silicon reactive infiltration is a manufacturing technique in which a carbon bound porous body, usually called ''preform'', is infiltrated with silicon in the liquid or vapor phase which, through an in situ chemical reaction, converts into silicon carbide. Si-SiC ceramics were first obtained by Hillig et al. [1] by infiltrating carbonaceous material with molten Si in vacuum (10^{-2} mbar) at temperatures ranging from 1450 °C and 1600 °C.

The related chemical reaction [2] is:

$$Si_{liquid} + C_{solid} = SiC_{solid} [\Delta H = -73 \ \text{kJ mol}^{-1}] \quad (1)$$

At these temperatures molten Si first infiltrates the porous carbon body by capillarity then reacts with it. In Ceramic Matrix Composite (CMC) manufacturing, this process is usually known as Melt Infiltration (MI) or Liquid Silicon Infiltration (LSI) [3].

Si-SiC CMC, are well known for their good thermo-mechanical properties [3] and are one of the few CMC ''mass products'' (e.g. ceramic brakes, furnace parts) on the market. The ''price to pay'' is for the presence of unreacted silicon (5–15 vol%) percolated into the structure. Indeed, in order to allow molten Si to fully infiltrate the preform in reasonable time, the volume of its porosity must be higher than the volume of silicon necessary for the stoichiometric reaction with carbon [4]. Si-SiC are fully dense materials and thus are oxidation resistant, but their use is limited by their working temperatures [5–6].

For applications at higher temperatures other ceramics, usually known as ultra high temperature ceramics (UHTCs), are used including the transition metal diborides of group IV [8]. ZrB_2 and HfB_2 have been widely studied for their high melting points, hardness, chemical and thermal stabilities [7]. Zirconium diboride can be of great interest in some applications

* Corresponding author.
E-mail address: alberto.ortona@supsi.ch (A. Ortona).

0272-8842/$36.00
doi:10.1016/j.ceramint.2011.12.030

(e.g. aerospace) not only because of its lower density with respect to hafnium diboride. ZrB_2 powders have been densified into compact bodies by hot pressing, pressureless sintering, reactive routes and spark plasma sintering [9,10]. In general these processes involve the use of expensive equipment, because of the processing conditions, and present limitations in product shaping. ZrB_2 has also been processed with additives to tailor its properties; among these, silicon carbide is one of the most widely employed [9,10]. The flexural strength and thermal conductivity of ZrB_2 ceramics can be increased by adding SiC particles [10,28]. ZrB_2-SiC ceramics can maintain the ''protective'' passive oxidation regime over a wide range of temperatures. Adding SiC (up to 30 vol%) to ZrB_2 not only extends the oxidation temperature range, thanks to the protective behavior of the formed mixed oxide scale [20], but it also allows the ceramic to rapidly regain its protective behavior if scale detaches during excessive temperature exposure [10]. Peng et al. [29] showed that higher concentrations of SiC resulted in thinner glassy surface layers, with lower concentrations of embedded zirconia, and thinner zirconium oxide under layers which could be beneficial or detrimental, depending on the application.

There are few works in the literature which try to produce ZrB_2-SiC based ceramics with alternative routes and they are mainly targeted at producing ceramic matrices for CMCs [11,12].

To the authors knowledge, literature reports two studies that explore ''mild processes'' in order to obtain dense Si-SiC-ZrB_2 composites at relatively a low temperature (1500 °C) and under pressureless conditions. Blum et al., using molten silicon reactive infiltration [13], developed thick UHTC protective coatings on top of lightweight C-SiC, SiC-SiC, and C-C fiber reinforced ceramics. Zhou et al. produced coatings on C/C composites by vapor silicon infiltration [14].

In this paper we propose a methodology to produce Si-SiC-ZrB_2 bulk ceramics, taking advantage of the reactive infiltration technique. Preforms with different contents of SiC and ZrB_2 were compacted with phenolic resin, pyrolysed and finally infiltrated with molten silicon at temperature above its melting point. The process was intentionally kept as simple as possible in order to maximize its cost efficiency.

Following the historical path of Si-SiC ceramics our long term goal is, starting from this work, to develop Si-SiC-ZrB_2 ceramic matrix composites by silicon reactive infiltration.

2. Experimental methods

In order to study how the SiC/ZrB_2 volume ratios affect composite manufacturing steps and the resulting microstructure, three different constituent compositions were prepared for this study. The compounds were compacted, pyrolysed in an inert atmosphere, and further infiltrated in vacuum with molten silicon.

2.1. Materials

The ceramic powders employed in this work were:

- α-Silicon carbide (Grade UF15 Stark Ag, D) with an average particle size d50 of 0.55 μm by Laser Diffraction and a specific area of 14–16 m^2/g
- Zirconium diboride (grade A Stark Ag D) average particle size d50 of 0.3–5.0 μm by Laser Diffraction.

The powders were pre-mixed to obtain a bimodal particle size distribution [28].

To produce the green bodies, a micronized (∼64 μm diameter) phenolic novolac powder (Hexion, USA) was mixed with the powders.

Samples were mixed maintaining a constant ratio between the solid charge (powders) and the plastic binder (phenolic resin). For the solid charge, three SiC-ZrB_2 powder mixtures were prepared (Table 1). Pyrolysed samples presented a similar porosity volume because the ratio of ceramic powders and phenolic resin was kept equal. A volume of around 50% of phenolic resin allowed compact-enough green and self-standing pyrolysed porous body with a sufficient amount of glassy carbon [15,16] to be prepared.

2.2. Green forming

The powders and phenolic resin were first dried separately in a vacuum oven for 30 min at 40 °C and 50 mbar residual pressure. First the solid charge was dry mixed for 30 min by slow ball milling in a sealed container, then milling was continued for a further 30 min with phenolic powder. The compound was immediately hot pressed with a uniaxial press for 150 s at 180 °C and at a pressure of 56 MPa. In plane dimensions the die and thus the sample was 90 × 40 mm^2.

Table 1
SiC (ρ = 3.21 g/cm^3), ZrB_2 (ρ = 6.10 g/cm^3 phenolic resin ratios for the produced samples.

Sample	Solid content (V%)				Binder (V%)
	51.44				48.56
	SiC (V%)		ZrB_2 (V%)		Phenolic resin (V%)
	On powder content	On total	On powder content	On total	
S100	100	51.44	0	0	48.56
S50Z50	50	25.72	50	25.72	48.56
S25Z75	25	12.86	75	38.58	48.56

The amount of powder put into the die was calculated in order to produce green performs 4–5 mm thick.

This first set of samples was over packed to be successfully infiltrated with Si. After pyrolysis, silicon was not able to infiltrate these bodies even for long dwelling times. In a second set, samples were then pressed under the same conditions with the exception of the temperature, which was lowered to 60 °C. At this temperature phenolic resin becomes more plastic than liquid. This allowed the compaction of green bodies which, after pyrolysis, were porous enough to be fully silicon infiltrated.

2.3. Pyrolysis

Green samples were pyrolysed in an electrical furnace inside a steel retort under inert atmosphere. During pyrolysis argon was injected into the retort at 300 SCCM. The heat ramp is reported in Table 2.

After pyrolysis, samples were then measured, weighted and new volume fractions calculated (Table 3). The plain phenolic resin carbon yield was 70% while the other powders were unaffected by this thermal treatment. An overall volumetric shrinking was similar for all the samples (5–7%). The apparent density was then calculated dividing the new mass by the new volume. These values were then used to calculate samples porosity.

It is worth of notice that the bodies did not crumble during pyrolysis, keeping high mechanical resistance after this processing step.

2.4. Silicon reactive infiltration

After pyrolysis, samples were placed on a boron nitride painted graphite plate. Carbon wicks were placed between the samples and the plate, to drain excess molten silicon. Silicon flakes were placed onto the samples. The amount of silicon was much higher than needed to react with phenolic derived carbon and to infiltrate the remaining porosity. However, based on our experience, this is necessary to fully infiltrate the preforms. Silicon infiltration was performed at 1500 °C with a 10^{-2} [mbar] residual pressure. The furnace was quickly brought to process temperature and held at that temperature for 2 h. The excess silicon reacted with the wicks or remained outside the sample as per Fig. 1.

Table 2
Pyrolysis heat ramp.

Temperature (°C)	Temperature rate (°C/h)	Ramp time (h)	Total time (h)
21–500	40	11	11
500–1000	60	8	19
1000	Dwell	1	20
1000–21	Power OFF	∼24	∼44

Table 3
Constituent materials calculated volume fractions.

Sample	ZrB_2%	SiC%	Res. carbon%	Porosity%
S100	0	38.3	15.0	46.7
S50Z50	18.8	19.2	15.9	46.3
S25Z75	31.6	10.6	19.4	38.2

2.5. Machining

Sample plates (Fig. 1) were first ground with a diamond mill on the outer surfaces, their thickness was consequently reduced in order to be sure to have a genuine Si-SiC-ZrB_2 system on the outer surface. The samples were then cut with a diamond saw into several pieces for characterization.

2.6. High temperature oxidation

In order to compare oxidized Si-SiC-ZrB_2 with other works [13,14,30,31], specimens were oxidized in a resistance heated tubular furnace at atmospheric pressure. They were placed in an alumina boat which was then positioned at the centre of an alumina tube. The furnace was brought to 1500 °C with an heating rate of 10 °C/min and held at that temperature for 2 h. A dry air flow of 200 SCCM was maintained in the furnace during the tests.

2.7. Characterization

Samples were characterized by several techniques.

Vickers microhardness measurements were carried out with a microdurometer (Leitz Wetzlar D). Microstructure evaluations on both oxidized and non-oxidized samples were performed with a Field Emission Scanning Electron Microscope (FESEM Zeiss Supra 25 D). Phase analysis was performed, during micrographs acquisition, with a Scandium 5.0 Soft Imaging System GmbH. XRD data were collected with a Philips PW3830 X-ray generator system.

3. Results and discussion

The following are the results of an initial characterization study aiming at evaluating Si-SiC-ZrB_2 properties and compairing them with a Si-SiC (S100) compound produced with the same methodology and with literature data. Si-SiC-ZrB_2 oxidation behavior was compared with similar systems adopted as protective coatings [13,14] and with ZrB_2-SiC [32–34].

3.1. Microstructure

Sample fracture surfaces after pyrolysis were analyzed by SEM. Well dispersed ZrB_2 powder is clearly visible as well as residual carbon around the big pores (Fig. 2a). Much finer SiC powders, in an agglomerate state (Fig. 2b) are present, while they are hardly discernible inside the pyrolysed carbon. Samples show a twofold pore size: bigger pores (Fig. 2c)

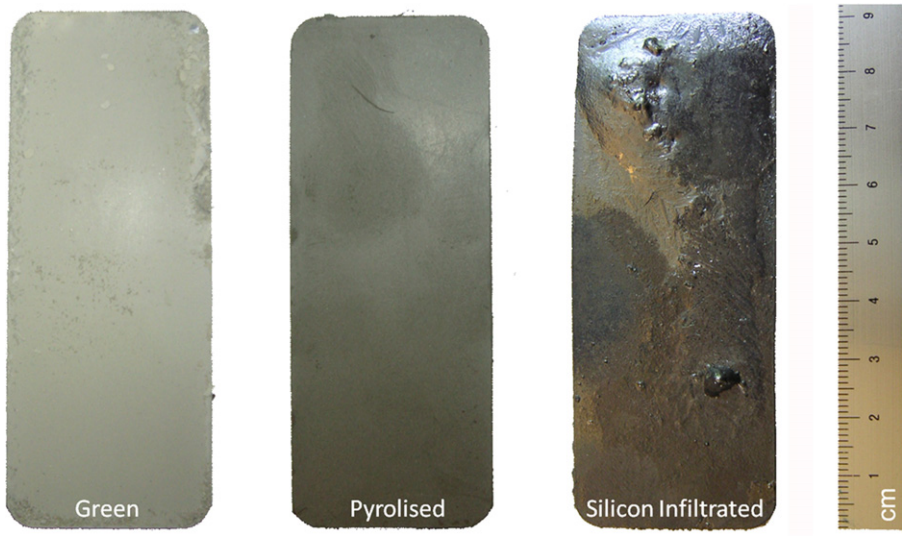

Fig. 1. Samples during processing steps.

correspond to the volume formerly occupied by the phenolic powders, smaller pores to the intra particle porosity. It was this bimodal porosity which allowed the silicon infiltration of rather thick (4–5 mm) samples. During the pyrolysis step the phenolic decomposed byproducts filled the intra particle porosity, keeping the ceramic body compact.

The patterns in Fig. 3 shows the crystalline phases detected by the instrument in the Si infiltrated samples. As expected, in S100 both silicon and silicon carbide are present. S50Z50 and S25Z75 samples show three crystal phases, namely: silicon, silicon carbide and zirconium diboride. Their presence is confirmed by micro hardness measurements whose data are reported in Table 4. Average results are lower than ZrB_2-SiC systems [17,18], due to the presence of silicon, while the hardness of each phase is in good agreement with literature data [19].

Fig. 4 shows the microstructures of S100, S50Z50 and S25Z75 samples after reactive silicon infiltration. Micrographs confirm the tendency of the SiC powders to agglomerate, due to the powder size and the fabrication method. Agglomeration is the cause of the small size pores clearly visible in Fig. 4(a and c).

The micrographs were taken in back-scattered electrons (BSE) mode to enhance the contrast between each phase. In Fig. 4(a) two phases with different gray tones are distinguishable, while in Fig. 4(b and c) a third white phase appears. An Energy-dispersive X-Ray spectroscopy (EDS or EDX) analysis on these three phases revealed that the light gray zones are made of Si, the dark gray zones of SiC and the white grains of ZrB_2. A further confirmation of the phases present in the samples comes from the elemental mapping reported in Fig. 5 for the S25Z75 sample. Furthermore, the interfaces between the

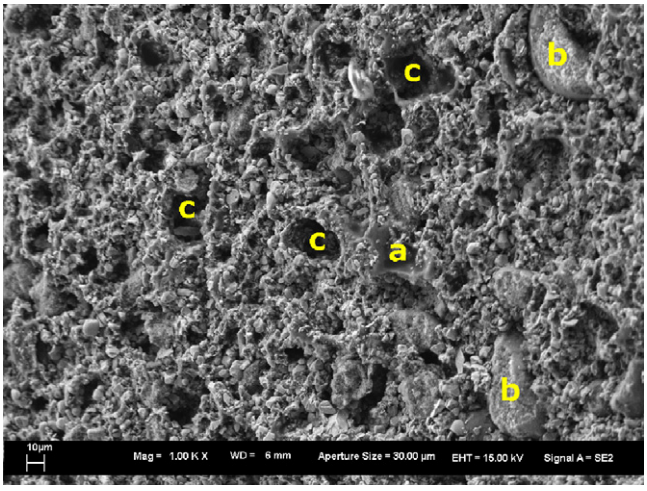

Fig. 2. S25Z75 sample after pyrolysis (fracture surface). Beside the dispersed ZrB_2 which is visible throughout the fracture surface, the micrograph shows (magnification: 1000×, voltage: 15 kV, working distance: 6 mm, aperture size: 30 µm): (a) glassy carbon, (b) SiC powders agglomerates and (c) big pores.

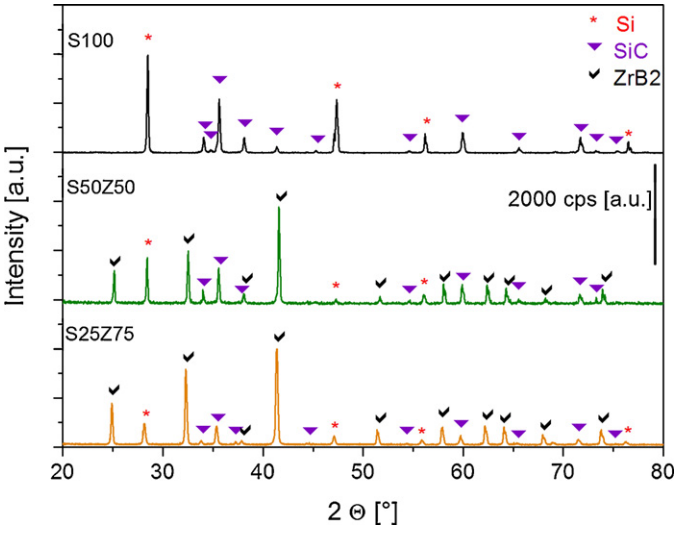

Fig. 3. XRD Patterns of S100, S50Z50 and S25Z75 sample, respectively.

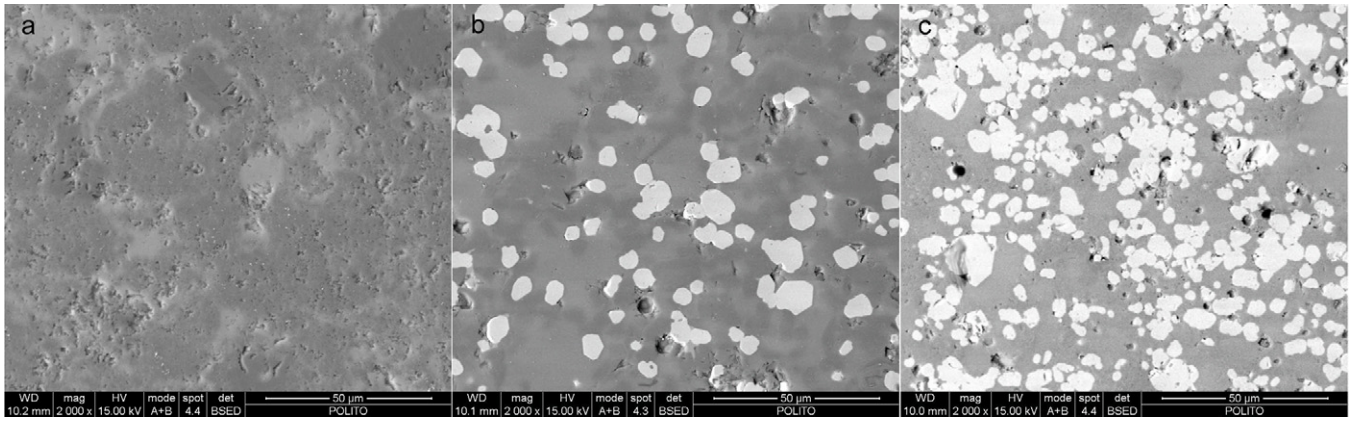

Fig. 4. SEM images of S100 (a), S50Z50 (b) and S25Z75 (c) obtained with back scattered electrons.

Table 4
Vickers micro hardness (load 300 g).

Sample	Multiphase indentations		Single phase indentations		
	Average value (GPa)	SD (GPa)	Si (GPa)	SiC (GPa)	ZrB_2 (GPa)
S100	16.2	3.2	9.9	24.0	–
S50Z50	17.6	0.8	9.5	26.1	15.6
S25Z75	14.2	2.4	9.3	24.2	14.0

different phases, especially for ZrB_2 compared with the rest of the matrix, are well defined.

XRD patterns in Fig. 3 and the micrographs in Fig. 4(b and c) also show that, during molten infiltration, silicon did not react with ZrB_2 although it formed SiC with the polymer derived carbon.

Silicon infiltrated the porous preforms regardless what SiC to ZrB_2 amounts into the solid charge was. Phenolic derived

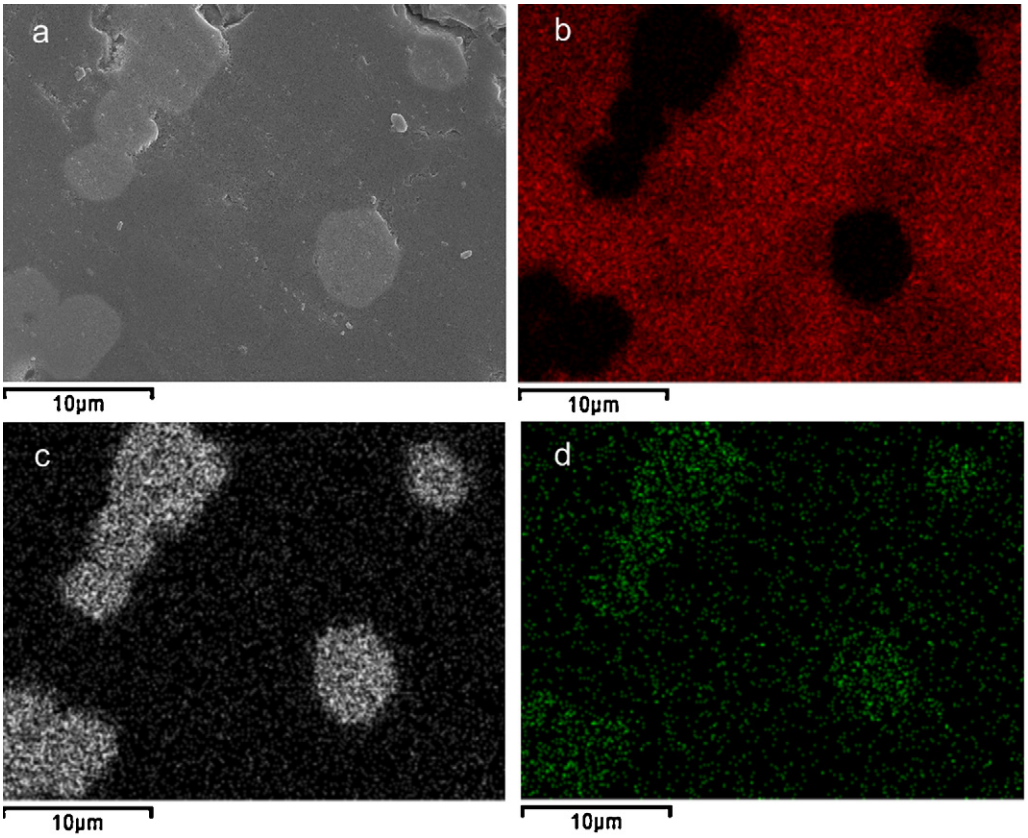

Fig. 5. Maps of the elements (b) silicon = red, (c) zirconium = white, (d) boron = green present on the detail SEM image of sample S25Z75.

Table 5
Literature contact angles of molten silicon on constituent materials.

Surface material	Equilibrium contact angle ϑ [°] of molten silicon		
Unreacted glassy carbon	>120 [22,23]		
Reacted glassy carbon	10–40 [23]	40–50[a] [21]	35–40 [22]
Reacted graphite	3–35[a] [23]	5–15[b] [21]	
SiC	38.5 ± 2[c] [24]	30[d] [21]	38[d], 41.5[e] [26]
ZrB_2	15[f] [25]		

[a] Depending on surface roughness.
[b] Pyrolitic graphite.
[c] α-SiC.
[d] Sintered.
[e] β-SiC.
[f] Datum is referred to TiB_2.

Table 6
Calculated phase volume fractions and overall densities on a ideally fully infiltrated sample. Measured density and estimated porosity.

Sample	Theoretical				Experimental	
	SiC phase (%)	ZrB_2 phase (%)	Si phase (%)	$\rho_{theor.}$ (g/cm^3)	ρ_{exp} (g/cm^3)	Porosity
S100	61.7	0	38.3	2.87	2.75	4.2%
S50Z50	43.8	18.8	37.4	3.43	3.30	3.8%
S25Z75	41.0	31.6	27.4	3.88	3.85	0.8%

carbon was the real ''bottle neck'' in terms of wetting since it presents poor wetting properties before reacting with silicon and forming SiC. When SiC is formed, all Si contact angles, measured on bulk specimens, are quite similar (Table 5). There are no data available on silicon wetting onto ZrB_2. The suggestion [27] of assuming a wetting behavior similar to TiB_2 for ZrB_2 (Table 5) was carried out. This hypothesis was confirmed by the weight gains during reactive infiltration and by the morphology analysis in Fig. 4(b and c) in which it is evident that silicon wrapped the ZrB_2 particles. Infiltration was somehow hindered by SiC powder agglomeration (Fig. 4(a and c)) since intra particle gaps were smaller inside the agglomerates.

Table 6 shows the phase volume percentages calculated from Table 4. SiC volume was calculated as the sum of the α-SiC powders and the SiC formed by reaction bonding between glassy carbon and Si. Values in Table 6 take into account the fact that the porosity, after silicon infiltration, was completely filled by unreacted Si.

Considering that, during reactive infiltration, carbon and Si became SiC as per Eq. (1), given the densities of SiC, ZrB_2 (Table 1) and Si ($\rho = 2.33$ g/cm^3), it was possible to calculate Si-SiC-ZrB_2 theoretical density and, after samples real density measurements, to estimate porosity.

3.2. Oxidation behavior

Fig. 6 shows the SEM analysis of the Si-SiC specimens (S100). From a morphological point of view, a continuous 20–30 μm external layer can hardly be detected, but it becomes evident if oxygen mapping is performed (Fig. 6b). Even at higher magnifications (Fig. 6d) the interface between oxidized and un-oxidized material is undistinguishable without the help of the oxygen map (Fig. 6e), meaning that the external oxidized layer is well adherent. The composition of the oxidized layer is primarily SiO_2, according to EDS analysis.

Fig. 7 shows a SEM analysis of the specimen with the highest amount of ZrB_2 (S25Z75). Similarly to Fig. 6, it is rather difficult to distinguish an oxidized layer (Fig. 7a), but one does become evident with the help of an oxygen map (Fig. 7b). Scale thickness is around 20–30 μm and it is composed of two phases; ZrO_2 (phase 3) and SiO_2 (phase 4). It is possible to point out that the difference between ZrB_2 and ZrO_2 is distinguishable also by a morphological point of view: ZrB_2 particles have smooth contours while ZrO_2 particles in the oxidized material have irregular and broken contours.

Boron distribution is difficult to characterize due to the low sensitivity of energy-dispersive spectroscopy to light elements but, as suggested by the literature on UHTCs [29–31], boron is oxidized to B_2O_3 which together with SiO_2 forms a borosilicate glass that is reported to significantly increase the resistance to oxygen diffusion through the surface.

Several authors have reported that oxidation of ZrB_2-SiC at 1500 °C in air produces a structure that consists of four layers [32–35]:

1. continuous SiO_2 on the outer surface
2. ZrO_2 embedded in amorphous SiO_2
3. SiC-depleted and ZrB_2
4. unaffected ZrB_2–SiC

Conversely to these findings, our oxidized Si-SiC-ZrB_2 specimens showed two layers (Fig. 7):

1) ZrO_2 embedded in SiO_2 and B_2O_3
2) unaffected Si-SiC-ZrB_2

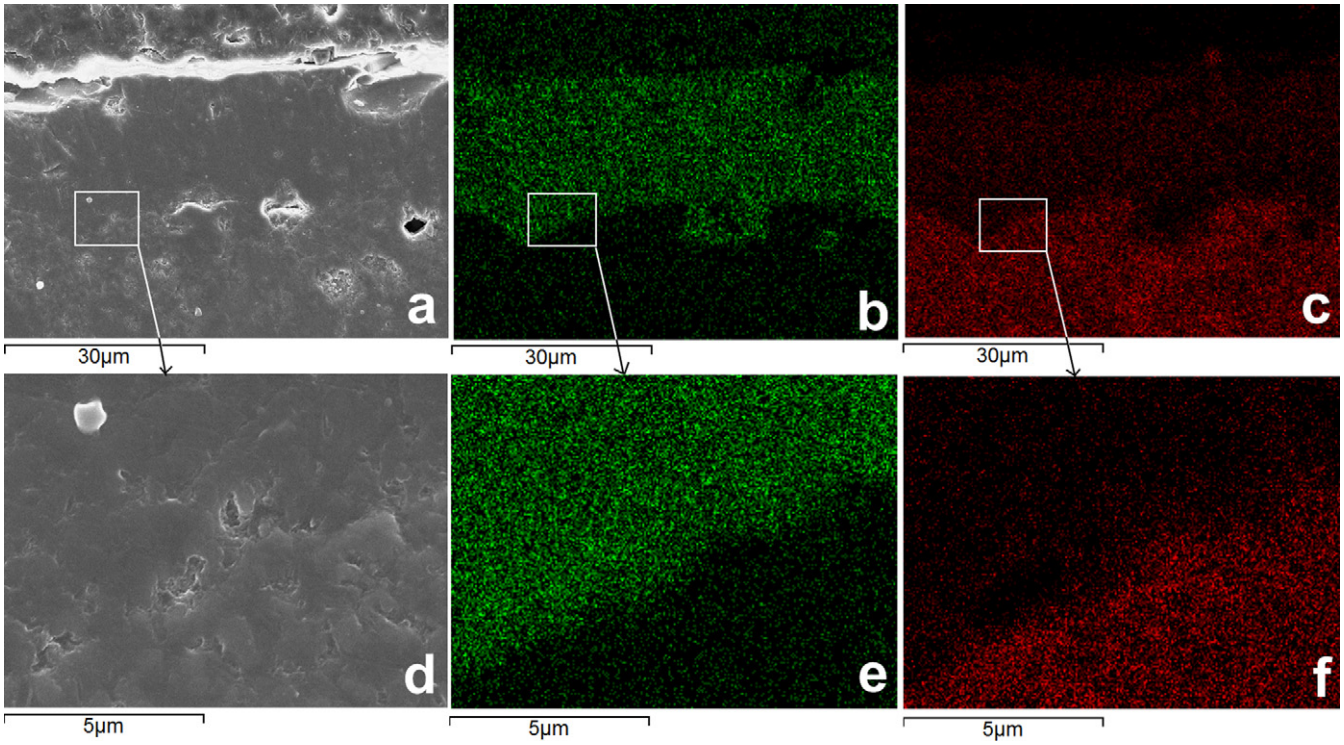

Fig. 6. SEM analysis of specimen S100 after oxidation. (a) General view with: (b) oxygen map, (c) silicon map. (d) Details of the interface between oxidized and un-oxidized material with: (e) oxygen map and (f) silicon map.

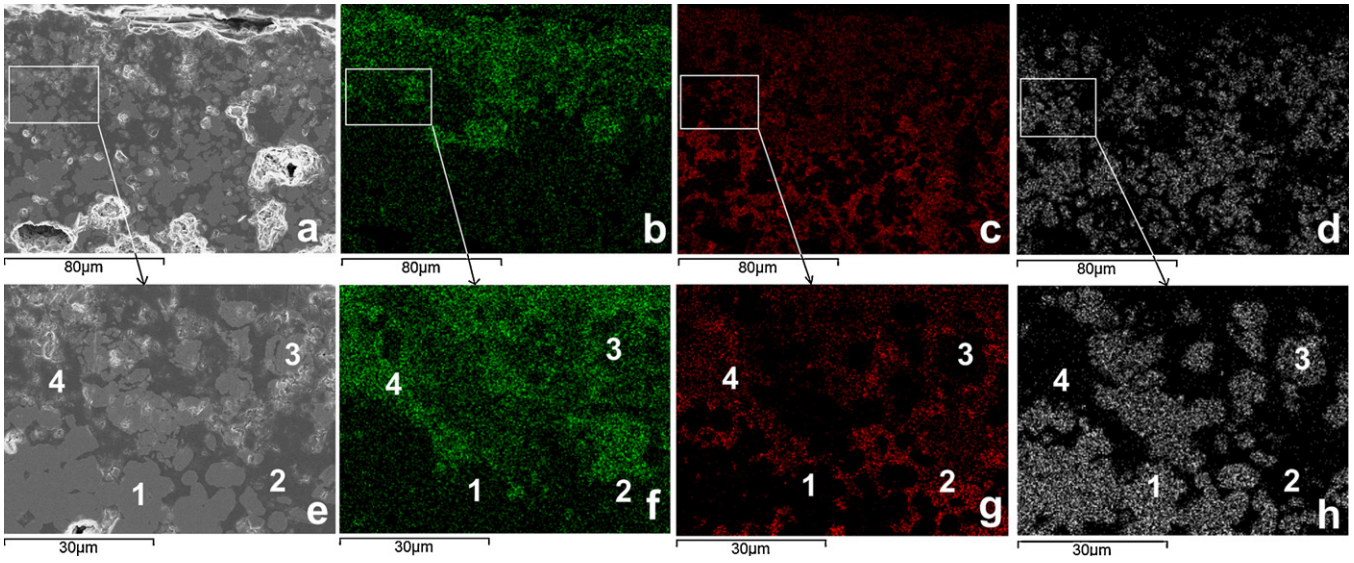

Fig. 7. SEM analysis of specimen S25Z75 after oxidation. (a) General view with: (b) oxygen map, (c) silicon map, (d) zirconium map. (e) Details of the interface between oxidized and un-oxidized material with: (f) oxygen map, (g) silicon map and (h) zirconium map.

These results are comparable with other Si-SiC-ZrB_2 systems employed as a protective coating [13,14] which were oxidized in similar conditions. Si-SiC-ZrB_2 systems differ from ZrB_2-SiC by the relative amount of SiC, which is much higher in Si-SiC-ZrB_2 and, of course, by the presence of unreacted silicon. An oxidation campaign is currently ongoing, in order to better understand Si-SiC-ZrB_2 oxidation behavior.

4. Conclusions

This work shows that Si-SiC-ZrB_2 composite bulks can be produced via silicon reactive infiltration. Although the process was kept as simple as possible in order to prove its cost efficiency, some features, like powder size selection and mixing, need to be improved in order to avoid powder

agglomeration. ZrB_2 powders did not react with molten silicon and remained a separate phase within the composite system. Preform porosity of samples after pyrolysis was intentionally kept at ~50% to ease Si infiltration. These high values affect the corresponding quantity of unaffected silicon after reactive infiltration. Further work will focus on reducing preform porosity and Si quantity.

Oxidized Si-SiC-ZrB_2 presented a double layer structure:

1) ZrO_2 embedded in SiO_2 and B_2O_3
2) unaffected Si-SiC-ZrB_2

The SiO_2 and B_2O_3 layer seems to act as a better oxygen barrier for the unaffected material. The typical SiC depleted region, present in oxidized ZrB_2-SiC materials, was not observed in this study.

References

[1] W.B. Hillig, R.L. Mehan, C.R. Morelock, V.J. DeCarlo, W. Laskow, Silicon/silicon carbide composites, Am. Ceram. Soc. Bull. 54 (12) (1975) 1054–1056.
[2] M.W. Chase Jr., NIST-JANAF themochemical tables, fourth edition, J. Phys. Chem. Ref. Data (1998) 1–1951 (Monograph 9).
[3] B. Heidenreich, in: W. Krenkel (Ed.), Melt infiltration Process in Ceramic Matrix Composites, vol. 113–119, Wiley-VCH, 2008.
[4] Y. Wang, S. Tan, D. Jiang, The effect of porous carbon preform and the infiltration process on the properties of reaction-formed SiC, Carbon 42 (2004) 1833–1839.
[5] N.S. Jacobson, Corrosion of silicon-based ceramics in combustion environments, J. Am. Ceram. Soc. 76 (1) (1993) 3–28.
[6] C.E. Ramberg, W.L. Worrell, Oxygen transport in silica at high temperatures: implications of oxidation kinetics, J. Am. Ceram. Soc. 11 (2001) 2607–2616.
[7] M.J. Gasch, D.T. Ellerby, S. Johnson, Ultra high temperature ceramic composites, in: N.P. Bansal (Ed.), Handbook of Ceramic Composites, Springer US, 2005, pp. 197–224.
[8] R.A. Cutler, Engineering Properties of Borides, in ASTM Engineered Materials Handbook, vol. 4 – Ceramics and Glasses, Schneider, S.J., technical chairman, pp. 787–803, 1991.
[9] W.G. Fahrenholtz, G.E. Hilmas, I.G. Talmy, J.A. Zaykoski, Refractory diborides of zirconium and hafnium, J. Am. Ceram. Soc. 90 (5) (2007) 1347–1364.
[10] S. Guo, Densification of ZrB2-based composites and their mechanical and physical properties: a review, J. Eur. Ceram. Soc. 29 (2009) 995–1011.
[11] N. Padmavathi, K.K. Ray, J. Subrahmanyam, P. Ghosal, S. Kumari, New route to process uni-directional carbon fiber reinforced (SiC + ZrB_2) matrix mini-composites, Mater. Sci. 44 (2009) 3255–3264.
[12] H. Hu, Q. Wang, Z. Chen, C. Zhang, Y. Zhang, J. Wang, Preparation and characterization of C/SiC-ZrB2 composites by precursor infiltration and pyrolysis process, Ceram. Int. 36 (2010) 1011–1016.
[13] Y.D. Blum, J. Marschall, D. Hui, S. Young, Thick protective UHTC coatings for SiC-based structures: process establishment, J. Am. Ceram. Soc. 91 (5) (2008) 1453–1460.
[14] H. Zhou, L. Gao, Z. Wang, S. Dong, ZrB_2-SiC oxidation protective coating on C/C composites prepared by vapor silicon infiltration process, J. Am. Ceram. Soc. 93 (4) (2010) 915–919.
[15] S.J. Wheeler, J. Sibold, I. Reimans, The effect of carbon on the processing of SiC/SiCf composites, in: J.P. Singh, N.P. Bansal, M. Singh (Eds.), Advances in Ceramic Matrix Composites VIII, John Wiley & Sons, 2002, pp. 43–53.
[16] C.A. Nannetti, A. Borello, D.A. de Pinto, D. Carbone, A. Licciulli, A. Ortona, C Fiber Reinforced Ceramic Matrix Composites by a Combination of CVI, PIP and RB, in: W. Krenkel, R. Naslain, H. Schneider (Eds.), High Temperature Ceramic Matrix Composites, Wiley-VCH Verlag GmbH & Co. KGaA, Weinheim, 2006, pp. 368–374.
[17] S.C. Zhang, G.E. Hilmas, W.G. Fahrenholtz, Mechanical properties of sintered ZrB2-SiC ceramics, J. Eur. Ceram. Soc. 31 (2011) 893–901.
[18] S.C. Zhang, G.E. Hilmas, W.G. Fahrenholtz, Pressureless sintering of ZrB2-SiC ceramics, J. Am. Ceram. Soc. 91 (1) (2008) 26–32.
[19] http://www.schunk-sik.com/en/schunk01.c.9111.de/all_productarticle.
[20] W.G. Fahrenholtz, Thermodynamic analysis of ZrB_2-SiC oxidation: formation of a SiC-depleted region, J. Am. Ceram. Soc. 90 (2007) 143–148.
[21] T.J. Whalen, A.T. Anderson, Wetting of Sic, Si_3N_4, and Carbon by Si and Binary Si Alloys, J. Am. Ceram. Soc. 58 (1975) 396.
[22] O. Dezellus, S. Jacques, F. Hodaj, N. Eustathopulos, Wetting and infiltration of carbon by liquid silicon, J. Mater. Sci. 40 (2005) 2307–2311.
[23] J.-G. Li, H. Hausner, Reactive wetting in the liquid-silicon/solid-carbon system, J. Am. Ceram. Soc. 79 (1996) 873.
[24] C. Rado, S. Kalegeropoulou, N. Eustathopulos, Wettingand adhesion in metal–silicon carbide systems: the effect of surface polarity of SiC, Scripta Mater. 42 (2000) 203–208.
[25] G.V. Samsonov, A.D. Panasiuk, M.S. Boriskova, Wettability of Group IV Metal Borides by Molten Metals, Smachivaemost Poverrkh. Svoistva Rasplavov Tverd. Tel–Naumka Dumka-Kiev, 1972.
[26] P. Nikolopoulos, S. Agatho Pou Los, G.N. Angelopoulos, A. Naoumidis, H. Grübmeier, Wettability and interfacial energies in SiC-liquid metal systems, J. Mater. Sci. 27 (1) (1992) 139–145.
[27] A. Passerone, personal communication, July 13, 2008.
[28] E. Eakins, D.D. Jayaseelan, W.E. LEE, Toward oxidation-resistant ZrB_2-SiC ultra high temperature ceramics, Metall. Mater. Trans. A 42A (2011) 878–887.
[29] F. Peng, Y. Berta, R.F. Speye, Effect of SiC, TaB_2 and $TaSi_2$ additives on the isothermal oxidation resistance of fully dense zirconium diboride, J. Mater. Res. 24 (5) (2008) 1855–1867.
[30] A.D.D. Jayaseelan, W.E. Lee, Toward oxidation-resistant ZrB_2-SiC ultra high temperature ceramics, Metall. Mater. Trans. A 42A (2011) 878–887.
[31] A. Rezaie, W.G. Fahrenholtz, G.E. Hilmas, Evolution of structure during the oxidation of zirconium diboride–silicon carbide in air up to 1500 °C, J. Eur. Ceram. Soc. 27 (2007) 2495–2501.
[32] W.G. Fahrenholtz, Thermodynamic analysis of ZrB_2-SiC oxidation: formation of a SiC-depleted region, J. Am. Ceram. Soc. 90 (1) (2007) 143–148.
[33] E.J. Opila, S. Levine, J. Lorincz, Oxidation of ZrB_2- and HfB_2-based ultra-high temperature ceramics: effect of Ta additions, J. Mater. Sci. 39 (2004) 5969–5977.
[34] M. Gasch, D. Ellerby, E. Irby, S. Beckman, M. Gusman, S. Johnson, Processing, properties, and arc jet oxidation of hafnium diboride/silicon carbide ultra high temperature ceramics, J. Mater. Sci. 39 (2004) 5925–5937.
[35] E.J. Opila, M.C. Halbig, Oxidation of ZrB_2-SiC, Ceram. Eng. Sci. Proc. 22 (2001) 221–228.